

PAPER • OPEN ACCESS

Numerical modelling of an electric motor cooling jacket

To cite this article: M Grespan *et al* 2024 *J. Phys.: Conf. Ser.* **2685** 012016

View the [article online](#) for updates and enhancements.



PRIME
PACIFIC RIM MEETING
ON ELECTROCHEMICAL
AND SOLID STATE SCIENCE

HONOLULU, HI
Oct 6–11, 2024

Abstract submission deadline:
April 12, 2024

Learn more and submit!

Joint Meeting of

The Electrochemical Society
•
The Electrochemical Society of Japan
•
Korea Electrochemical Society

Numerical modelling of an electric motor cooling jacket

M Grespan¹, L Campanelli¹, D Angeli² and R Freddi³

¹ DISMI - Dipartimento di Scienze e Metodi dell'Ingegneria, Università di Modena e Reggio Emilia, Via Amendola 2, Pad. Buccola, 42122 Reggio Emilia (Italy)

E-mail: mattia.grespan@unimore.it

² Centro Interdipartimentale EN&TECH, Piazzale Europa 1, 42124 Reggio Emilia (Italy)

³ Fira Spa, Strada Statale 255, 374/B, 44047 Dosso Terre del Reno, Italy

Abstract. The automotive industry is amid a sweeping change of propulsion technology to meet the increasingly stringent limits on emissions and fuel consumption. Traditional combustion engines are gradually being replaced by electric motors or hybrid power trains. The efficiency and power density levels achievable by electric motors are entirely dependent on the effectiveness of the employed cooling solution. Therefore, extensive analyses are needed to determine and optimise the thermal performance of these systems. In this work a numerical model is developed to determine the friction losses and the heat transfer properties of an electric motor cooling jacket. The cooling channels, which coil along the circumferential direction within the motor casing, are studied by means of CFD analysis of a basic periodic module. Flow and temperature fields are determined by applying a 3D Finite Volume approach. Numerical solutions are obtained by means of a validated conjugate heat transfer solver. Integral flow field results are employed to derive the equivalent Darcy friction factor and side-wall specific Nusselt numbers for several flow regimes. A lumped parameter thermal model, based on the graph theory and aforementioned CFD results is also developed to determine the overall system performance. The equivalent thermal resistances are computed from geometric parameters and CFD results. Finally preliminary numerical results on friction losses and heat transfer are compared with available experimental data.

Keywords: electric motor, cooling jacket, forced convection, CFD, lumped parameter model, RANS

1. Introduction

Electric motors are increasingly being employed for automotive traction, due to more and more stringent standards on fuel consumption and pollutant emissions. The design and optimization of the cooling solution for electric motors is of utmost importance, as it strongly affects the achievable efficiency and power levels. Traditionally, thermal analysis of electric machines is carried out by means of thermal resistance models, whereas the use of more advanced numerical techniques such as computational fluid dynamics and finite element analysis is still limited.

One of the most relevant works on the development of lumped parameter models is that of Mellor *et al.* [1], in which the authors developed a thermal resistance network based on a general hollow cylindrical component, considering radial and axial conduction. Kral *et al.* [2] and Aglén *et al.* [3], developed similar models for water cooled electric machines, using empirical correlations to derive the convective heat transfer coefficients. Nategh *et al.* [4] performed simple



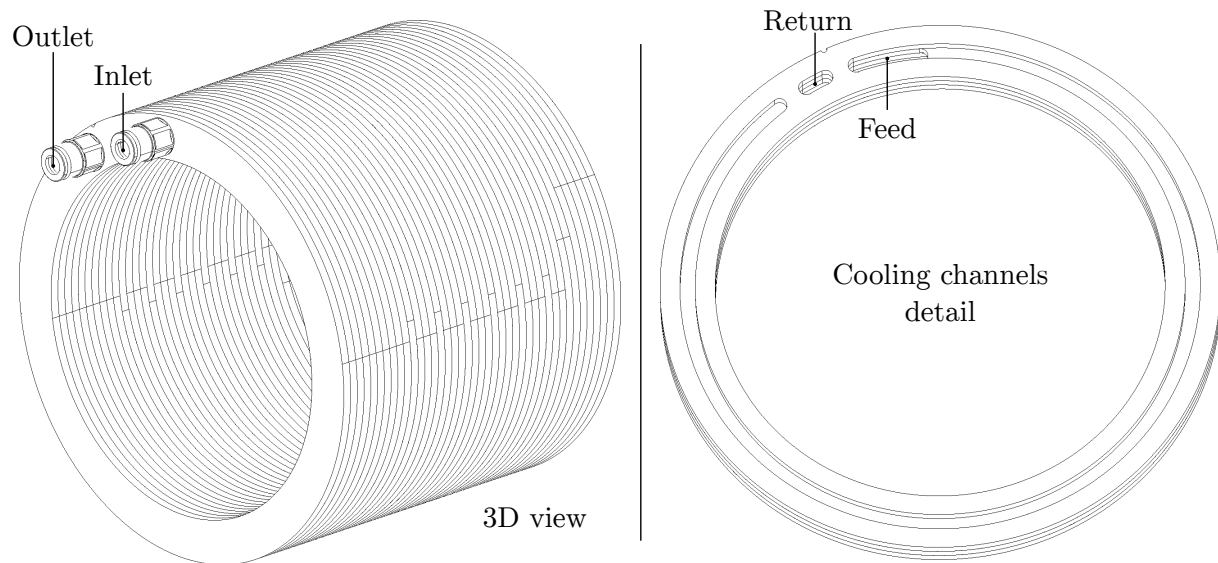


Figure 1. External geometry of the motor casing under examination (left), and a set of plates that clearly show the geometry of the feed and return channels (right).

CFD analyses to determine coolant flow distribution through the housing channels, and on the end winding surfaces. The resulting velocity values were then used to calculate the heat transfer coefficients, by employing empirical relationships.

In this work, a multiscale approach for the fluid dynamic and thermal analysis of an electric motor cooling jacket is presented. The cooling channels, which evolve in steps along the circumferential direction, are analysed by developing a CFD model for a periodic channel module under fully developed flow conditions. Numerical results on head losses and heat transfer, presented in terms of equivalent Darcy friction factor and sidewall-specific Nusselt numbers, are used to derive suitable correlations. A lumped parameter thermal model is also presented, with aim of studying the temperature distribution in the entire cooling jacket. The thermal resistances are determined from geometric parameters, physical principles, and the aforementioned correlations.

Preliminary global results on head losses and heat transfer, based on a simplified version of the model are compared with available experimental results and prior numerical studies.

2. Case study

This study is focused on an aluminum electric motor casing, constructed by stacking and brazing aluminium plates, which feature machined slots. This production process yields motor casings with great mechanical strength and cooling channels with intricate geometries, achieved by staggering and stacking several slotted plates. In this case, coolant flows along the casing circumference, reversing the direction when passing from one channel to the next. Then, coolant flows back towards the outlet port, positioned on the same side as the inlet, through a straight axial return channel. The motor casing features internal and external diameters of 147 and 183 mm, respectively. The slots constituting the cooling channels have a width of 5 mm and are positioned on the mean circumference. The axial length is 152 mm. Figure 1 shows a drawing of the cooling jacket, with a detail of the internal cooling channels, which are obtained by alternating plates with slots covering different angular spans.

3. Numerical model of the feed channel

Fluid flow and heat transfer analysis about the cooling jacket feed channel is conducted by means of CFD techniques. The geometry is divided into periodic modules which are repeated along the cooling jacket axis. Each module consists of the fluid and solid regions associated with a full turn of the cooling channels, so that the inlet and outlet sections are vertically aligned. The steady-state, incompressible, and fully developed flow and thermal fields about the unitary module are determined from the numerical solution of RANS and energy equations.

$$\begin{cases} \nabla \cdot (\vec{v} \otimes \vec{v}) = -\frac{1}{\rho} \nabla p + \nabla \cdot [(\nu + \nu_t) \nabla \vec{v}] + \sigma \\ \nabla \cdot \vec{v} = 0 \\ \nabla \cdot (\rho \vec{v} h) + \nabla \cdot \left(\rho \vec{v} \frac{|\vec{v}|^2}{2} \right) = -\nabla \cdot \vec{q} + \nabla \cdot (\vec{\tau} \cdot \vec{v}) \end{cases} \quad (1)$$

Temperature in solid regions is determined from the Laplace equation:

$$\nabla^2 T = 0. \quad (2)$$

Eddy viscosity is determined by means of the $k-\omega$ SST turbulence model [5]. The momentum source term σ in Eqs. (1) stands for the external forcing needed to maintain the desired flow rate at the channel vents. The channel height y is chosen as the problem reference length, and it is used to scale down the computational domain. The flow is defined on the channel height based Reynolds and Prandtl numbers. Mean velocity over inlet and outlet sections, fluid density, and thermal conductivity are set to unitary reference values. Under the selected dimensionless framework the fluid dimensionless kinematic viscosity and specific heat are:

$$\mu^* = \nu^* = \frac{1}{\text{Re}} \quad c_p^* = \text{Re Pr}. \quad (3)$$

Dimensionless properties of solid regions are derived by scaling the thermophysical properties of aluminum by the ones of the adjacent fluid.

$$\lambda_s^* = \frac{\lambda_{\text{alu}}}{\lambda_{\text{fluid}}} \quad (4)$$

A fully developed flow solution is attained by enforcing periodic conditions between the inlet and outlet patches. At all fluid-solid interfaces no-slip conditions are applied to velocity and a zero-gradient condition is assigned to pressure; finally, continuity of temperature and heat fluxes is enforced.

Heat transfer effectiveness of the geometry under examination is evaluated by deriving an equivalent heat transfer coefficient for each sidewall of the channel. To this end, six sidewall specific sets of boundary conditions for wall temperature are defined: a uniform entering heat flux is applied to the sidewall under investigation, while all other walls are assumed adiabatic.

Numerical solution of the governing equations is obtained by means of a Finite Volume conjugate heat transfer solver based on the SIMPLE algorithm, and implemented in the OpenFOAM computational suite [6]. Advective terms are discretized by means of second-order upwind schemes. Instead, central schemes featuring explicit non-orthogonality correction are used for diffusive terms.

The computational domain consists of a conformal hybrid mesh, whose selected views are shown in Fig. 2, in which fluid and solid regions are clearly highlighted. In addition, a numeric ID is assigned to each sidewall for future reference.

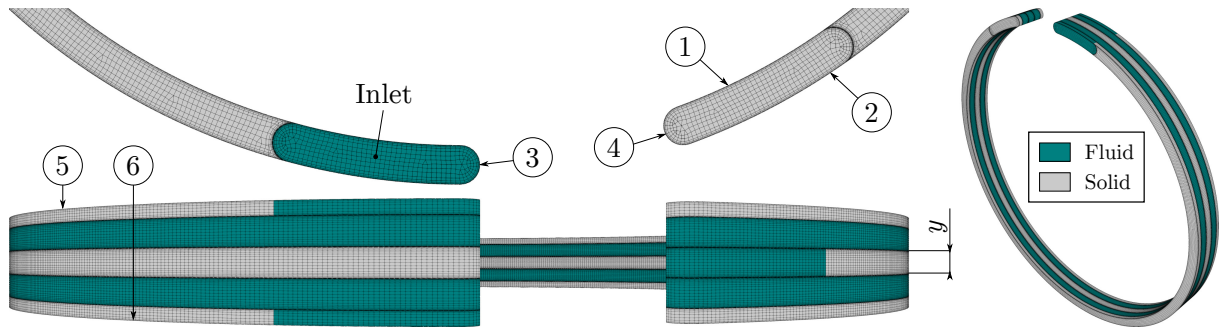


Figure 2. Selected views of the feed channel computational grid, along with identification of each sidewall via a numeric ID.

4. Lumped parameter thermal model

In the following a lumped parameter thermal model is presented, to determine the temperature distribution within aluminium walls, and the heat flux between feed and return channels. The motor casing is again divided in axial periodic modules, each of which includes the periodic feed channel section analysed in §3, a portion of the return channel, and the associated aluminium walls. Each periodic module is then divided into a set of hollow cylindrical sectors. The schematic of figure 3a shows the subdivision into sectors of a periodic casing module: the blue region represents the feed channel, thus includes the fluid and solid regions constituting the CFD model discussed in §3; the red region stands for the portion of the axial return channel associated with the periodic module, while aluminium walls are depicted in white.

The generic cylindrical sector is modelled by a network formed by seven nodes and six thermal resistances, under the assumption that the centre temperature defines heat flow along the radial, circumferential, and axial directions, and that the heat fluxes are independent of each other. In a solid region, the centre point temperature θ represents the average temperature of the aluminium section, while in fluid regions T_0 stands for the average bulk temperature between inlet and outlet sections.

4.1. Solid element

The six thermal resistances that make up a generic solid cylindrical element are calculated on the basis of the conduction shape factor S and the average thermal conductivity λ_a [7]:

$$R_{ij} = \frac{1}{S_{ij} \lambda_a} . \quad (5)$$

The cylindrical conduction shape factors are computed from geometric parameters following the general approach proposed by Yovanovich [8].

$$S_{01} = \frac{l \vartheta}{\ln(r_2/r_1)} \quad (6)$$

$$S_{02} = \frac{l \vartheta}{\ln(r_3/r_2)} \quad (7)$$

$$S_{03} = S_{04} = \frac{2l \ln(r_3/r_1)}{\vartheta} \quad (8)$$

$$S_{05} = S_{06} = \frac{\vartheta (r_3^2 - r_1^2)}{l} \quad (9)$$

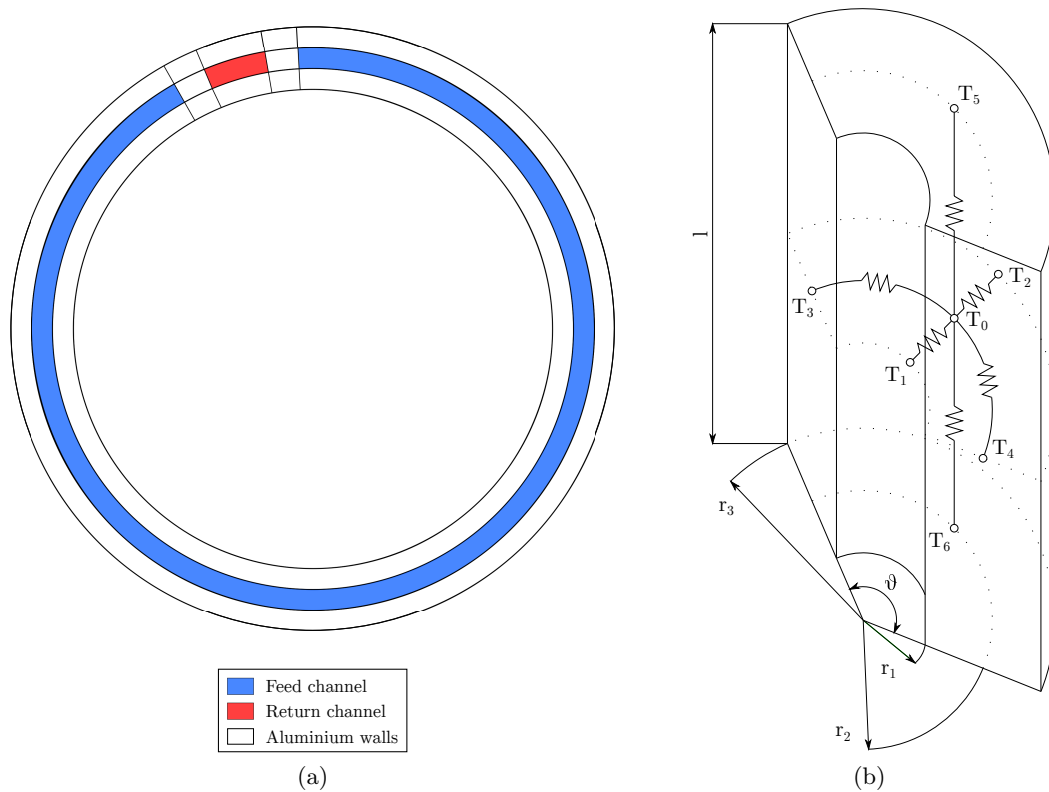


Figure 3. Schematics showing the set of cylindrical sectors constituting a casing periodic module (a), and the arrangement of nodes and thermal resistances modelling heat flux within a single cylindrical sector (b).

4.2. Feed channel

The feed channel is modeled by a thermal resistance network similar to the one depicted in Fig. 3b, with the addition of two nodes standing for the inlet and outlet bulk temperatures. The convective thermal resistance between the centre node, and each sidewall is derived from the classical relationship:

$$R_{ij} = \frac{1}{h_{ij} A_{ij}}, \quad (10)$$

where h_{ij} is determined from the CFD developed Nusselt number correlations presented in §5. The equivalent resistance between the centre node and the nodes associated with inlet and outlet bulk temperatures is given by:

$$R_{\text{blk}} = \frac{1}{\dot{m} c_p}. \quad (11)$$

4.3. Return channel

The return channel is represented by a seven-node thermal network in which the bottom and top nodes stand for the inlet and outlet bulk temperatures, respectively. The convective heat transfer coefficient is assumed uniform and determined from the Dittus–Boelter correlation

$$\text{Nu}_D = 0.023 \text{Re}_D^{4/5} \text{Pr}^n. \quad (12)$$

The resistances associated with the bulk temperature nodes are obtained from Eq. 11.

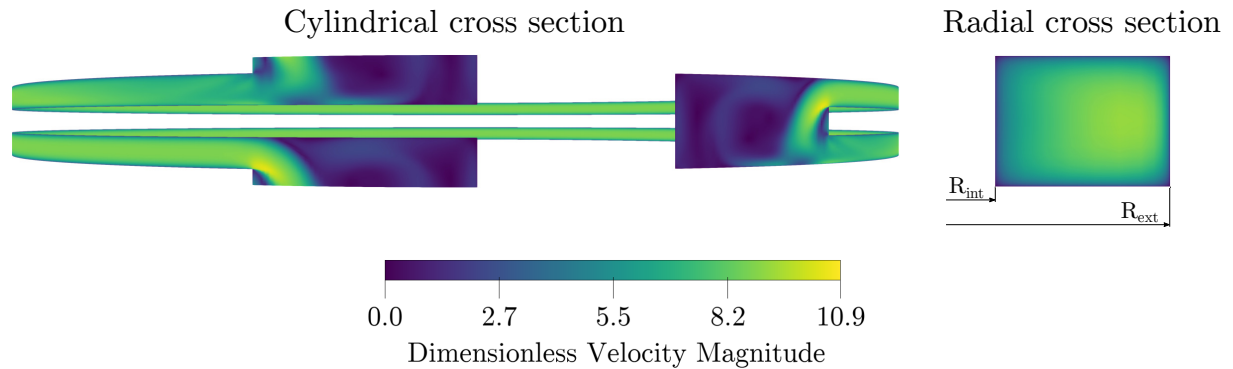


Figure 4. Colour maps of dimensionless velocity magnitude on cylindrical and radial sections, at $Re=1800$ and $Pr=7$.

5. Results

5.1. Feed channel

Flow field results are presented by means of dimensionless velocity colour maps about a radius-centred cylindrical section, and a radial cross section, shown in Fig. 4. At the intersection between two circumferential channels the flow turns sharply forming a small separation bubble on the inside of the turn. Subsequent impingement and flow redistribution on the channel base lead to a local high velocity region which improves heat transfer effectiveness. In the connecting region between the channels overall low fluid velocity leads to poor local heat transfer performance, as will be shown later. In the radial velocity section (Fig. 4) the effects of centrifugal forces are clearly spotted, as fluid velocity is greater towards the external side of the channel. The observed flow pattern leads to major head losses and decreased heat transfer effectiveness in the connecting region between channels, this is also confirmed by the integral results presented in the following.

Integral results on head losses and heat transfer effectiveness consist of an equivalent Darcy friction factor and wall-specific Nusselt numbers. The equivalent friction factor is derived from the Darcy-Weisbach formula, employing the external forcing term σ :

$$f = \frac{2 \sigma y}{\rho \bar{u}_1^2}, \quad (13)$$

where \bar{u}_1^2 is integral mean velocity over the inlet section. The Nusselt number related to the i -th channel sidewall is derived from the classic convection thermal resistance definition:

$$Nu_i = \frac{q'' y}{\lambda (\bar{T}_{w,i} - \bar{T}_b)}. \quad (14)$$

In Eq. (14) $\bar{T}_{w,i}$ stands for the surface mean temperature over the i -th sidewall, while \bar{T}_b is the average bulk temperature between the inlet and outlet sections. Finally, q'' is the heat flux entering at the wall. Numerically derived f and Nu values are employed to derive Reynolds number based correlation functions:

$$f = -1.373 \times 10^5 Re^{5.038 \times 10^{-4}} + 1.380 \times 10^5, \quad (15)$$

$$Nu = c_1 Re^{c_2} + c_3. \quad (16)$$

The c_i coefficients in Eq. (16), related to a single Prandtl number ($Pr=7$), are reported in Tab. 1. Figure 5 shows the numerical f and Nu values along with the related correlation functions. The

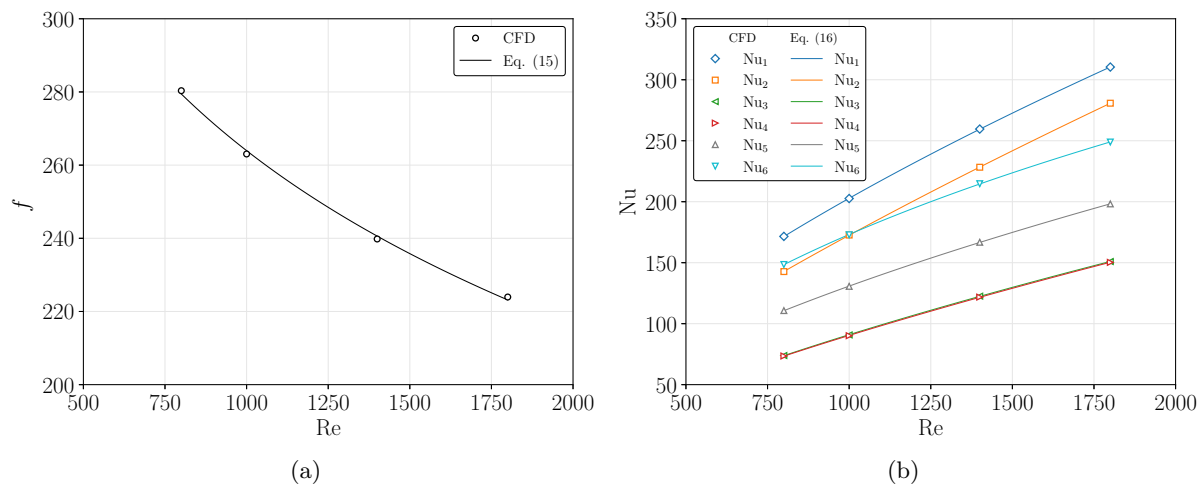


Figure 5. Numerical results and the associated correlations for the equivalent Darcy friction factor (a), and Nusselt numbers related to each sidewall of the feed channel (b).

internal and external walls feature the highest Nusselt number values out of the six side walls, as at these walls most of the heat flux is applied directly to the fluid. The difference between the upper and lower Nusselt number values suggests the existence of an axial heat flux within the cooling jacket; this deviation is due to the previously discussed flow pattern in the connecting region between channels.

Finally, the lowest Nu -values are found for the two walls facing the return channel, due to the low velocity separated flow. In this case, a small heat transfer coefficient is beneficial, as it prevents heat from the return channel to enter. Finally, these two sidewalls feature an identical thermal behaviour, meaning that one less CFD simulation would be needed for each Reynolds number.

5.2. Preliminary results on overall head losses and heat transfer

In the following preliminary results on head losses and heat transfer are compared with available experimental data. Overall head losses are evaluated using the Darcy-Weisbach formula and deriving the friction factor value from Eq. (15). At a flow rate of 3 l/min of a water-glycol solution the numerically obtained head losses are 16% higher than the experimental ones, which

Table 1. Values of c_i coefficients in Eq. (16).

Sidewall ID	c_1	c_2	c_3
1	2.769	0.643	-31.75
2	0.862	0.778	-14.0
3	1.103	0.681	-30.96
4	0.858	0.710	-25.44
5	3.040	0.579	-35.49
6	23.67	0.372	-136.9

is considered acceptable.

A simplified version of the lumped parameter model presented in §4, which considers only the convective heat transfer at the feed channel internal wall, is used to obtain the inner wall temperature. The calculated temperature exceeds the reference value by 3.3 K; a slight overestimation is expected, as heat transfer with the external ambient air is not taken into account.

6. Conclusions

A multiscale modelling methodology for an electric motor cooling jacket was presented in this work. Cooling channels featuring a stepped circumferential geometry were studied by developing a CFD model. Numerical results were presented and discussed. Integral results on head losses and heat transfer were employed to derive correlation functions for the equivalent Darcy friction factor and sidewall-specific Nusselt number. A thermal resistance model was also presented to study the temperature distribution within the entire cooling jacket. Preliminary results based on a simplified version of the aforementioned model were compared with available experimental data showing a promising accuracy.

The developed approach can of course be applied to motor casings having cooling channels of any geometry. Furthermore, if circumferential periodicity of the cooling channels can be exploited the number of nodes of the lumped parameter model can be significantly reduced, allowing for a faster and more convenient implementation.

Future research efforts will be focused towards completing the development of the lumped parameter model and on the investigation of different fluids and flow regimes.

Acknowledgments

The research has been partially funded under the National Recovery and Resilience Plan (NRRP), Project "Sustainable Mobility Center (Centro Nazionale per la Mobilità Sostenibile - CMNS)", Project code CN00000023 - CUP E93C22001070001.

References

- [1] PH Mellor D Roberts D T Lumped parameter thermal model for electrical machines of tefc design 1991 *IEE proc., Electr. power appl.* **138**(5) 205–218(13)
- [2] Kral C, Haumer A and Bauml T Thermal model and behavior of a totally-enclosed-water-cooled squirrel-cage induction machine for traction applications 2008 *IEEE Trans. Ind. Electron.* **55** 3555–3565
- [3] Aglen O and Andersson A 2003 Thermal analysis of a high-speed generator *38th Conf. Rec. Ind. Appl. Soc. IEEE-IAS Annu. Meet.* vol 1 pp 547–554 vol.1
- [4] Nategh S, Huang Z, Krings A, Wallmark O and Leksell M Thermal modeling of directly cooled electric machines using lumped parameter and limited cfd analysis 2013 *IEEE Trans. Energy Convers.* **28** 979–990
- [5] Menter F Two-equation eddy-viscosity turbulence models for engineering applications 1994 *AIAA J.* **32** 1598–1605
- [6] Weller H G, Tabor G, Jasak H and Fureby C A tensorial approach to computational continuum mechanics using object-oriented techniques 1998 *Comput. phys.* **12** 620–631
- [7] Incropera F P and DeWitt D P 2006 *Fundamentals of Heat Transfer* (Wiley)
- [8] YOVANOVICH M A general expression for predicting conduction shape factors 1973 *11th Aerosp. Sci. Meet.*